Dynamical Transitions from Slow to Fast Relaxation in Random Open Quantum Systems

Dror Orgad,[1] Vadim Oganesyan,[2,3] and Sarang Gopalakrishnan[4]

[1]*Racah Institute of Physics, The Hebrew University, Jerusalem 91904, Israel*
[2]*Department of Physics and Astronomy, College of Staten Island, CUNY, Staten Island, New York 10314, USA*
[3]*Center for Computational Quantum Physics, Flatiron Institute, 162 5th Avenue, New York, New York 10010, USA*
[4]*Department of Electrical and Computer Engineering, Princeton University, Princeton, New Jersey 08540, USA*

We explore the effects of spatial locality on the dynamics of random quantum systems subject to a Markovian noise. To this end, we study a model in which the system Hamiltonian and its couplings to the noise are random matrices whose entries decay as power laws of distance, with distinct exponents α_H, α_L. The steady state is always featureless, but the rate at which it is approached exhibits three phases depending on α_H and α_L: a phase where the approach is asymptotically exponential as a result of a gap in the spectrum of the Lindblad superoperator that generates the dynamics, and two gapless phases with subexponential relaxation, distinguished by the manner in which the gap decreases with system size. Within perturbation theory, the phase boundaries in the (α_H, α_L) plane differ for weak and strong decoherence, suggesting phase transitions as a function of noise strength. We identify nonperturbative effects that prevent such phase transitions in the thermodynamic limit.

The dynamics of generic quantum systems has been a central theme in contemporary many-body physics, spanning disciplines from quantum information to condensed matter and high-energy physics. A key conceptual tool in this context is random matrix theory (RMT), which prescribes studying systems governed by dynamics that is as random as is allowed by the symmetries and other constraints of the underlying problem of interest. RMT has been used over the past four decades to study quantum chaos in closed systems that lack spatial structure [1,2]. Recently, various extensions of RMT that include forms of spatial structure were considered. These range from banded random matrices [3] (which represent generic local *single-body* problems), to random circuits [4] (which represent random many-body problems with no structure beyond the spatial locality of interactions), and the SYK model [5] (in which interactions are *few body* but not otherwise local). Such explorations have led to a deeper understanding of quantum chaos, entanglement dynamics, and related questions.

Despite some early applications of RMT to *open* quantum systems [6–9], studies of systems whose Hamiltonian and couplings to a Markovian bath are drawn from RMT ensembles have only recently appeared [10–22]. A notable conclusion that has emerged is that such fully nonlocal open systems are rapidly equilibrating, i.e., the spectrum of their Lindblad superoperator is generically *gapped* in the thermodynamic limit. This conclusion is supported by numerical evidence, exact solutions, and general bounds [12,13]. In contrast, one does not expect a gap in the opposite limit of local dissipative dynamics where the slowest-relaxing modes are long-wavelength spatial

probability fluctuations, which decay through diffusion. For many-body systems with few-body interactions, the connectivity graph is more complicated but is still local in Fock space, hence suggesting a gapless Lindbladian, consistent with numerics [16]. The discrepancy between the local and nonlocal regimes indicates that there must be a phase transition between them.

In this Letter we identify such phase transitions by exploring an ensemble of master equations constructed from power-law random banded matrices (PRBMs). PRBMs can be regarded as random hopping models in one dimension, with hopping that falls off as a power α of the distance between two sites [3,23–25]. They interpolate between conventional random matrices in the $\alpha \rightarrow 0$ limit and short-range hopping systems with power-law localized eigenvectors for large α. These models have been studied extensively in the Hamiltonian case [3], where a localization transition occurs at $\alpha = 1$. Here, we analyze related ensembles for *open* systems, whose Hamiltonian and couplings to a Markovian noise of strength γ are given by $N \times N$ PRBMs with two distinct powers α_H and α_L. We find a rich phase diagram, shown in Fig. 1, containing three dynamical phases: (i) a gapped phase in which the relaxation rate remains independent of N, (ii) a "hydrodynamic" phase where the relaxation rate falls off as a power law of N and the slowest-relaxing modes are long-wavelength fluctuations, and (iii) a "Lifshitz" phase where the relaxation rate falls off logarithmically in N, and the slowest-relaxing modes are localized perturbations in real space. Notably, we find that the limits $N \rightarrow \infty$ and $\gamma \rightarrow 0$ (or $\gamma \rightarrow \infty$) do not always commute, and finite-N systems
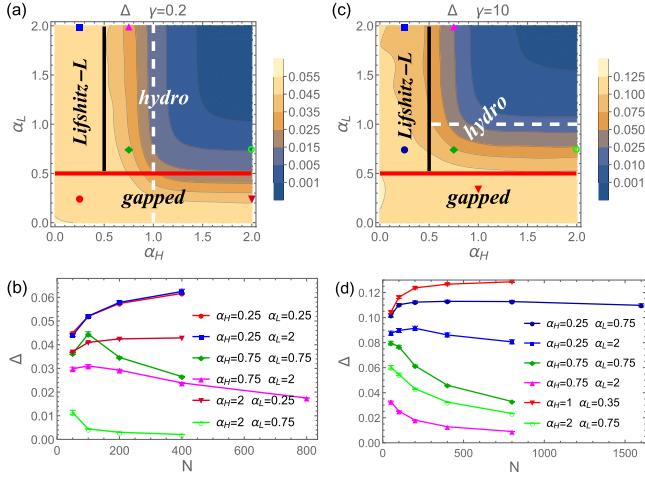
FIG. 1. (a) The Lindbladian spectral gap as a function of the exponents α_H, α_L at weak decoherence $\gamma = 0.2$ and $N = 100$. The solid lines mark the $N \to \infty$ phase transitions between gapped, hydrodynamic, and Lifshitz phases. The dashed line marks a change in the populations' content of the slowest decaying eigenvector. (b) N dependence of the gap for selected values of (α_H, α_L) indicated by colored symbols in (a). (c)–(d) Similar data at strong decoherence $\gamma = 10$.

with given (α_H, α_L) may exhibit quite different behaviors for small and large γ. However, we show that in the $N \to \infty$ limit the weak- and strong-decoherence regimes connect smoothly and any phase transitions as a function of γ (apart from the appearance of midgap states reported for the pure RMT case [12]) are avoided due to nonperturbative effects.

Model.—We consider systems described by noisy dynamics of the form $H(t) = H + \xi(t)L$, where ξ is a Gaussian Markovian noise with variance γ. The Hamiltonian H and the jump operator L are $N \times N$ random matrices [26], whose elements in the position basis are $G_{ij} f_{ij}$. Here, G is a matrix from the Gaussian orthogonal ensemble and $f_{ij} = 1/(\delta_{ij} + |i - j|^\alpha)$, where the exponent α generally takes different values, α_H and α_L, for H and L. We normalize G such that the variance of the spectrum of both H and L is $1/2$ for all α_H, α_L. The noise-averaged dynamics is described by the Lindblad master equation

$$\partial_t \rho = \mathcal{L}\rho \equiv -i[H, \rho] + \gamma(L\rho L - L^2\rho/2 - \rho L^2/2). \quad (1)$$

The eigenvalues of the Lindbladian superoperator $\mathcal{L}$ occupy the complex half-plane $\mathrm{Re}(\lambda) \leq 0$ and are either real or form complex conjugated pairs [12]. The steady state ($\lambda = 0$) of the specified model is always the maximally mixed state $\rho_0 = \mathbb{I}/N$. The remaining right eigenvectors of $\mathcal{L}$ are traceless matrices, ρ_i, $i = 1, \ldots, N^2 - 1$, that are either Hermitian or form Hermitian conjugated pairs. A general density matrix can be expanded as $\rho(t) = \rho_0 + \sum_{i=1}^{N^2 - 1}(a_i e^{\lambda_i t}\rho_i + \mathrm{H.c.})$ and its late-time approach to ρ_0 is governed by the eigenvalue with the smallest negative

real part, $-\Delta$, and its corresponding eigenvector ρ_1. (This is always true in finite systems, but important exceptions exist in the thermodynamic limit [27–29].) As $N \to \infty$, Δ may tend to a positive value (i.e., is "gapped") or approach zero ("gapless"), and we compute its dependence on α_H, α_L, and γ.

Overview of PRBMs.—We will invoke the spectral properties of PRBMs and thus briefly review their properties [3,30]. (i) For $\alpha < 1/2$, PRBMs are akin to structure-less random matrices: their eigenstates are random vectors and their eigenvalues follow a Wigner semicircle distribution. (ii) For $1/2 < \alpha < 1$, almost all eigenstates $|v\rangle$ are extended, as revealed by their inverse participation ratio (IPR) $I = \sum_{i=1}^N |v_i|^4$ that vanishes in the large-N limit. However, they typically exhibit sparse spatial structure spanning only a fraction of the sites. Concomitantly, the eigenvalue distribution becomes unbound due to Gaussian tails [25] consisting of states that are localized around potential extremes and are unable to find any resonances within the system. These tail states are subextensive in number but, as we will show, may dominate the late-time dynamics. (iii) For $\alpha > 1$, all eigenstates are localized with power-law decay $|v_i| \sim 1/i^\alpha$.

Rate equations: Small γ.—We begin by discussing the limit of small or large γ at finite N, where the analysis is facilitated by the ability to perturbatively eliminate all but N of the eigenvectors of $\mathcal{L}$. As noted above, the limits $\gamma \to 0, \infty$ and $N \to \infty$ do not always commute and we will address this issue later. Consider first the case $\gamma = 0$. Here, the eigenvectors of $\mathcal{L}$ are $|ij\rangle \equiv |i\rangle\langle j|$ with eigenvalues $i(E_i - E_j)$, where $H|i\rangle = E_i|i\rangle$. The N eigenvectors of the form $|ii\rangle$ have zero eigenvalue, i.e., are steady states. Following the convention in the NMR literature we dub them "H populations" and the other $N(N-1)$ states "H coherences." At first order in γ the noise does not couple populations and coherences, and one can write down classical rate equations for the populations [12], $\partial_t|ii\rangle = \sum_j A_{ij}|jj\rangle$, where

$$A_{ij} = \gamma(|\langle i|L|j\rangle|^2 - \delta_{ij}\langle i|L^2|j\rangle). \quad (2)$$

When $\alpha_H < 1/2$, the eigenbasis of H is effectively random, leading to rates A_{ij} that are approximately chi-squared distributed with a mean and a standard deviation that scale as γ/N. We have previously shown that such conditions lead to a gap $\Delta = \gamma/2$ [12]. Conversely, when $\alpha_H > 1$ the H eigenvectors are localized. Analytical progress can be made by modeling them as a set of power-law envelopes centered on each of the N sites (ignoring their mutual orthogonality) and by averaging A_{ij} over the statistics of L. Within this "mean-field" approximation A is similar to a Hamiltonian whose hopping amplitudes between sites i, j vary as $|i - j|^{-2\alpha'}$, where $\alpha' \equiv \min(\alpha_H, \alpha_L)$, and whose rows sum up to zero [30]. The mean-field analysis predicts a gap when $\alpha' < 1/2$, a

superdiffusive relaxation for $1/2 < \alpha' < 3/2$ with a lowest eigenvalue that vanishes as $N^{1-2\alpha'}$, and diffusive dynamics, where this eigenvalue vanishes as N^{-2} for $\alpha' > 3/2$. Solving the rate equations numerically yields a qualitatively similar behavior with a gapped phase for $\alpha_L < 1/2$ and a gapless phase for $\alpha_L > 1/2$, albeit with a slower decay of the lowest eigenvalue with N as compared to the mean-field prediction [30]. For $1/2 \leq \alpha_H \leq 1$ the typical eigenstates of H do not have a simple description. Our numerical results indicate a gapped phase for $\alpha_L < 1/2$ and a "weakly gapless" behavior for $\alpha_L > 1/2$, where ρ_1 is a localized population in the Lifshitz tail of H whose eigenvalue slowly decreases with N [30].

Rate equations: Large γ.—A similar analysis can be carried out at large γ [12]. Here, one begins by diagonalizing the dissipative part of $\mathcal{L}$, finding eigenvectors of the form $|\mu\nu\rangle = |\mu\rangle\langle\nu|$, with eigenvalues $-(\gamma/2)(\kappa_\mu - \kappa_\nu)^2$, where $L|\mu\rangle = \kappa_\mu|\mu\rangle$. Again, there are N eigenvectors with zero eigenvalue corresponding to "L populations." Eliminating their coupling to the remaining $N(N-1)$ "L coherences" to second-order in H leads to rate equations $\partial_t|\mu\mu\rangle = \sum_\nu A_{\mu\nu}|\nu\nu\rangle$ with transition rates

$$A_{\mu\nu} = \frac{4}{\gamma} \frac{|\langle\mu|H|\nu\rangle|^2(\kappa_\mu - \kappa_\nu)^2}{(\kappa_\mu - \kappa_\nu)^4 + (2/\gamma)^2(\langle\mu|H|\mu\rangle - \langle\nu|H|\nu\rangle)^2}. \quad (3)$$

Probability conservation enforces $A_{\mu\mu} = -\sum_{\nu\neq\mu} A_{\mu\nu}$. In the strict large-$\gamma$ limit at finite N, one would ignore the γ-dependent part of the denominator. However, this term regularizes the effective dynamics for all finite γ. Hence, we discuss Eq. (3) below and contrast it with the unregularized form in the Supplemental Material [30].

When $\alpha_L < 1/2$, the spectrum of L is *bounded* with extended states, causing H to act as a featureless random perturbation between L populations. Consequently, one can coarse-grain Eq. (3) in κ space and replace $|\langle\mu|H|\nu\rangle|^2$ by its average to find a gap $\Delta \simeq 2/\gamma$ [12,30]. For $1/2 < \alpha_L < 1$, most of the L eigenvectors are still delocalized. However, typical realizations of L also have spatially localized tail states whose eigenvalues are far from the rest of the spectrum of L. The matrix elements out of these tail states are suppressed according to Eq. (3). As a rough estimate, in a sample of size N the extremal eigenvalue resides approximately $\sqrt{\log N}$ away from the bulk of the spectrum [30]. ρ_1 is localized on this extremal state, and the gap closes logarithmically in system size. When $\alpha_L > 1$ the eigenvectors of L are localized and its spectrum is unbounded. Consider the case $\alpha_L = \infty$, where they are roughly localized on sites and the dominant dependence of $A_{\mu\nu}$ comes from $|\langle\mu|H|\nu\rangle|^2$, scaling as $|\mu - \nu|^{-2\alpha_H}$. For $\alpha_H < 1/2$, these elements fluctuate sufficiently weakly that one can still coarse grain [30]. Since the L spectrum is unbounded, tail states set a logarithmically decaying gap. For $\alpha_H > 1/2$ the effective hopping between L populations

is local, leading to hydrodynamic behavior with extended eigenvectors and a gap that decays as a power law with N. Numerically, we find that this behavior persists down to $\alpha_L = 3/2$, where the gap is again set by tail states [30].

Comparison of small and large γ.—We briefly summarize our findings using the rate equations. (a) When $\alpha_L < 1/2$, a gapped phase is predicted for all γ. (b) When α_H, α_L are both sufficiently large ($\alpha_H > 1$, $\alpha_L > 3/2$), a gapless phase is predicted for all γ. (c) Elsewhere, the rate equations for small and large γ yield incompatible results. For $\alpha_H < 1/2$, $\alpha_L > 1/2$ they suggest a gap-closing transition at finite γ, and in the remaining part of the (α_H, α_L) plane they disagree on the way the gap closes with increasing N. As we will argue, these discrepancies are absent for sufficiently large N.

Numerical investigation of $\mathcal{L}$.—We have contrasted the above predictions against the spectrum of the full Lindbladian (which is an $N^2 \times N^2$ matrix) for a relatively small system size $N = 100$, where a fine sweep across parameter space is feasible. We then examined larger systems of up to $N = 1600$ at selected points in the (α_H, α_L) plane. At these sizes, we do not have access to the full spectrum of $\mathcal{L}$ but we can find the leading two eigenvalues and their corresponding eigenvectors by the power method. The resulting phase diagrams (Fig. 1) match our expectations from the rate equations in regimes (a) and (b) specified above. In regime (c), we find behavior that lies beyond the rate equations.

A more sensitive probe than the gap is the nature of ρ_1. In the gapless regime we find that for small γ and N it follows the prediction of the rate equations and is extended both in the position and H eigenbases as long as $\alpha_H > 1$, while it is localized in both bases for $1 > \alpha_H > 1/2$ [30]. However, as N increases ρ_1 becomes delocalized in the entire $\alpha_H > 1/2$ gapless regime. One can characterize the failure of the rate equations by the fraction of the operator norm of ρ_1 that lies in the populations subspace. This is representing how well a population-only approximation (i.e., classical rate equation) can capture ρ_1. As shown by Supplemental Material, Fig. 4 [30] the overlap with the populations is large for $\alpha_H > 1$, but diminishes with N for $\alpha_H < 1$. Intuitively, one expects such behavior if ρ_1 is hydrodynamic at large N, with a population that is modulated *in real space*. Since the eigenstates of H are delocalized when $\alpha_H < 1$, the projectors onto them miss the real-space structure. By contrast, for $\alpha_H > 1$ the eigenstates are localized, so local populations in energy space are a good proxy for local populations in real space.

We now support this intuition by analyzing the case $\gamma \ll 1$, $\alpha_L = \infty$, $1/2 < \alpha_H < 1$, corresponding to a system subject to local noise and a Hamiltonian with power-law hopping and random on-site potentials. Consider a wave packet initially localized in real space. In the clean system, it hybridizes via coherent tunneling with states at all distance scales R, with a Rabi frequency $\sim R^{-\alpha_H}$. However,
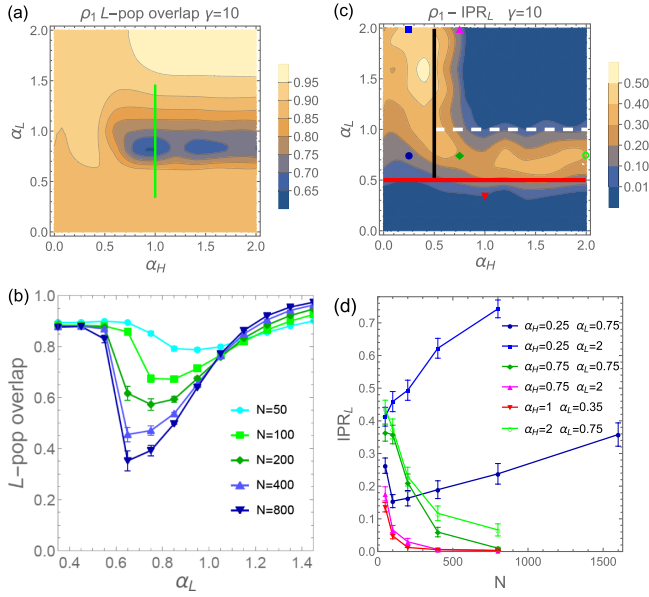
FIG. 2. (a) Overlap between ρ_1 and the L populations at strong decoherence $\gamma = 10$ and $N = 100$. (b) N dependence of the overlap along the cut shown in (a). L coherences are essential to describe the state when $\alpha_H > 1/2$ and $1 > \alpha_L > 1/2$. (c) The IPR of ρ_1 in the L eigenbasis. (d) N dependence of the IPR for the (α_H, α_L) values indicated in (c). ρ_1 is dominated by a tail L population when $\alpha_H < 1/2$, $\alpha_L > 1/2$.

local noise of strength γ sets a timescale γ^{-1} and a length scale $R_\gamma \sim \gamma^{-1/\alpha_H}$ beyond which coherent tunneling is disrupted. For $R > R_\gamma$ transport is governed by incoherent hopping processes with a rate that is set by Fermi's golden rule and scales as $1/R^{2\alpha_H}$. Since $2\alpha_H > 1$, incoherent hopping is *local* in this regime and the slow modes are accordingly hydrodynamic in real space. The eigenstates of H are the wrong basis because they are formed by delicate tunneling resonances that any amount of decoherence can disrupt. Evidently this argument extends to general $\alpha_L > 1$, and an exactly parallel argument can be made for large γ and $1/2 < \alpha_L < 1$.

ρ_1 remains delocalized for $\alpha_H > 1/2$ also in the strong-decoherence thermodynamic limit. This is apparent from Fig. 2, showing its IPR in the L-population subspace $\mathrm{IPR}_L = \sum_\kappa \rho_{\kappa\kappa}^4 / (\sum_\kappa \rho_{\kappa\kappa}^2)^2$, where $\rho_{\kappa\kappa}$ are its components within this subspace. Conforming to the prediction of the rate equations, the crossover regime $\alpha_H > 1/2$, $1 > \alpha_L > 1/2$ exhibits an eigenvector that is still largely concentrated on a population of a spatially localized L-tail state at small N. However, the IPR_L diminishes with N, and ρ_1 becomes modulated in real space. Hence, for similar reasons to those outlined above, its projection onto the L populations also vanishes, see Fig. 2. In contrast, the IPR_L increases with N when $\alpha_H < 1/2$, $\alpha_L > 1/2$. We have confirmed that this is a result of ρ_1 becoming more concentrated on a population of a localized L-tail state. Thus, we conclude that the range $\alpha_H < 1/2$, $\alpha_L > 1/2$ hosts a thermodynamic Lifshitz phase whose gap vanishes very slowly, as shown by Fig. 1.

Both the perturbative rate-equation analysis and the available numerical data point at a transition from a small-γ gapped phase to a large-γ weakly gapless Lifshitz phase when $\alpha_H < 1/2$ and $\alpha_L > 1/2$. Nevertheless, we argue that the $N \to \infty$ spectrum in this range is weakly gapless for all γ. The key observation is that the spectrum of H is bounded whereas that of L is unbounded. Hence, in the large-N limit, the largest energy scale is associated with the Lifshitz tail states of L and grows as $\sqrt{\log N}$. Consequently, as $N \to \infty$ the noise cannot be treated perturbatively. Rather, the tail states must be diagonalized out first, and only then can one apply the large-γ perturbation theory to treat their mixing with other states via H. The resulting gap diminishes as $1/(\gamma \log N)$ but is challenging to detect: since the fixed-N, $\gamma \to 0$ perturbation theory yields a gap of order γ the tail-state eigenvector extends below it only when $N > \exp(1/\gamma^2)$. For small γ this regime is numerically inaccessible. Instead, the Supplemental Material demonstrates small-γ Lifshitz behavior using a model whose density of L eigenvalues decays only as κ^{-4}.

Discussion.—Our Letter focused on the spectral gap Δ. To make contact with the dynamics of local observables we have followed the evolution of an initial state with $\rho_{ij} = (\delta_{ij} - \delta_{i1}\delta_{j1})/(N - 1)$. We observe an asymptotic exponential approach of every ρ_{ii} to the steady state value $1/N$. The relaxation time is Δ^{-1} at all sites i, but the onset time of the asymptotic approach varies with i and depends on the overlap $(\rho_1)_{ii}$ with the slowest mode [30]. At shorter times, the relaxation is faster, due to more rapidly decaying eigenstates. These points are demonstrated by Fig. 3 and the Supplemental Material [30]. In terms of the natural scale Δ^{-1} the asymptotic approach begins earliest in the hydrodynamic phase, then in the gapped phase and finally in the Lifshitz phase, where most sites have only algebraically small overlap with ρ_1.

Often, when classical noise controls the experiment, it couples to a single collective variable, e.g., the dipole moment of a chaotic quantum dot. Although we focused on this case, a more general setting involves multiple decoherence channels with their associated jump operators.
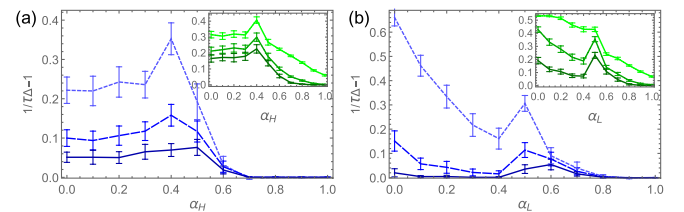

FIG. 3. (a) The relative difference between the spatial average of the relaxation rate τ^{-1} of local observables and Δ for $\gamma = 10$, $\alpha_L = 1.5$, and $N = 400$. The dotted, dashed, and solid lines are based on τ^{-1} extracted by fitting the relaxation over the range $t = 3$–6, 6–9, and 9–$12\Delta^{-1}$, respectively. The inset shows the standard deviation of the relative difference. (b) The same quantities as a function of α_L for $\alpha_H = 1.5$.

In the Supplemental Material we extend our treatment to systems with several PRBM jump operators with exponents α_{L_k} [30]. Let us briefly quote the results. When $\tilde{\alpha}_L = \min(\alpha_{L_k}) < 1/2$, the spectrum is gapped, otherwise it is gapless. A weakly gapless Lifshitz phase occurs when $\tilde{\alpha}_L > 1/2$ and $\alpha_H < 1/2$. Finally, when all exponents exceed $1/2$ we predict a hydrodynamic regime.

Our analysis found three distinct phases as a function of the decay exponents (α_H, α_L), but no phase transitions as a function of the decoherence strength γ. Our analysis is consistent with the possibility of transitions between gapped phases, as in Ref. [12]; indeed, we expect such transitions everywhere in the gapped phase $\alpha_L < 1/2$.

A natural question is whether the transitions we find exhibit nontrivial critical phenomena. While we have not addressed these in detail, our results shed some light on the matter. The transition from gapped to hydrodynamic relaxation as one tunes α_L at fixed $\alpha_H \gg 1$ and small γ is a transition purely in the decay rates of the hydrodynamic modes: the low-lying eigenvectors themselves evolve smoothly with α_L, and show no signs of a diverging length scale. The extended modes do change across the same transition at large γ, and further study is required. The α_H-tuned transition from Lifshitz to hydrodynamic relaxation at fixed $\alpha_L \gg 1$ appears rather simple: it is a level crossing between the localized Lifshitz tail state and the hydrodynamic mode, and as such shares some similarities with other spectral "first-order" transitions [31]. Finally, the transition between gapped and Lifshitz relaxation at $\alpha_H < 1/2$ as one tunes α_L through $1/2$ is a nontrivial critical point, associated with the emergence of tails in the density of states of PRBMs [3]. This transition is a particularly promising candidate for experimental studies in ion traps, which allow us to realize power-law couplings with tunable exponents [32].

[1] C. W. J. Beenakker, Rev. Mod. Phys. **69**, 731 (1997).

[2] L. D'Alessio, Y. Kafri, A. Polkovnikov, and M. Rigol, Adv. Phys. **65**, 239 (2016).

[3] A. D. Mirlin, Y. V. Fyodorov, F.-M. Dittes, J. Quezada, and T. H. Seligman, Phys. Rev. E **54**, 3221 (1996).

[4] M. P. A. Fisher, V. Khemani, A. Nahum, and S. Vijay, Annu. Rev. Condens. Matter Phys. **14**, 335 (2023).

[5] V. Rosenhaus, J. Phys. A **52**, 323001 (2019).

[6] R. Grobe and F. Haake, Phys. Rev. Lett. **62**, 2893 (1989).

[7] F. Haake and K. Życzkowski, Phys. Rev. A **42**, 1013(R) (1990).

[8] B. Mehlig and J. T. Chalker, J. Math. Phys. (N.Y.) **41**, 3233 (2000).

[9] Y. V. Fyodorov and H.-J. Sommers, J. Phys. A **36**, 3303 (2002).

[10] Z. Xu, L. P. García-Pintos, A. Chenu, and A. del Campo, Phys. Rev. Lett. **122**, 014103 (2019).

[11] S. Denisov, T. Laptyeva, W. Tarnowski, D. Chruściński, and K. Życzkowski, Phys. Rev. Lett. **123**, 140403 (2019).

[12] T. Can, V. Oganesyan, D. Orgad, and S. Gopalakrishnan, Phys. Rev. Lett. **123**, 234103 (2019).

[13] T. Can, J. Phys. A **52**, 485302 (2019).

[14] L. Sá, P. Ribeiro, and T. Prosen, J. Phys. A **53**, 305303 (2020).

[15] L. Sá, P. Ribeiro, and T. Prosen, Phys. Rev. X **10**, 021019 (2020).

[16] K. Wang, F. Piazza, and D. J. Luitz, Phys. Rev. Lett. **124**, 100604 (2020).

[17] S. Lange and C. Timm, Chaos **31**, 023101 (2021).

[18] W. Tarnowski, I. Yusipov, T. Laptyeva, S. Denisov, D. Chruściński, and K. Życzkowski, Phys. Rev. E **104**, 034118 (2021).

[19] V. Popkov and C. Presilla, Phys. Rev. Lett. **126**, 190402 (2021).

[20] J. L. Li, D. C. Rose, J. P. Garrahan, and D. J. Luitz, Phys. Rev. B **105**, L180201 (2022).

[21] L. Sá, P. Ribeiro, and T. Prosen, Phys. Rev. Res. **4**, L022068 (2022).

[22] A. Kulkarni, T. Numasawa, and S. Ryu, Phys. Rev. B **106**, 075138 (2022).

[23] A. D. Mirlin and F. Evers, Phys. Rev. B **62**, 7920 (2000).

[24] I. Varga and D. Braun, Phys. Rev. B **61**, R11859(R) (2000).

[25] O. Yevtushenko and V. E. Kravtsov, Phys. Rev. E **69**, 026104 (2004).

[26] We draw the matrices representing H and L in an uncorrelated way. Hence, they do not commute with probability 1. In case they commute, the Lindbladian $\mathcal{L}$ possesses N steady states given by the populations $|i\rangle\langle i|$, where $|i\rangle$ are the simultaneous eigenstates of H and L.

[27] S. Yao and Z. Wang, Phys. Rev. Lett. **121**, 086803 (2018).

[28] J. Bensa and M. Žnidarič, Phys. Rev. X **11**, 031019 (2021).

[29] T. Mori and T. Shirai, Phys. Rev. Lett. **130**, 230404 (2023), and references therein.

[30] See Supplemental Material at http://link.aps.org/supplemental/10.1103/PhysRevLett.132.040403 for additional details on the properties of PRBMs. We also include numerical data on the behavior of the populations' rate equations at weak and strong decoherence alongside an analytical treatment of their mean-field approximation. The Supplemental Material also contains results for a related model that exhibits a Lifshitz phase at weak decoherence, systems with multiple jump operators, and the dynamics of local observables.

[31] M. M. Parish, Phys. Rev. A **83**, 051603(R) (2011).

[32] P. Richerme, Z.-X. Gong, A. Lee, C. Senko, J. Smith, M. Foss-Feig, S. Michalakis, A. V. Gorshkov, and C. Monroe, Nature (London) **511**, 198 (2014).